International Journal of Biological Macromolecules 124 (2019) 1094–1105

Contents lists available at ScienceDirect

International Journal of Biological Macromolecules

journal homepage: http://www.elsevier.com/locate/ijbiomac

Mixed gels from whey protein isolate and cellulose microfibrils

Jinfeng Peng [a], Vincenzo Calabrese [a], William Nicholas Ainis [a], Ruben Scager [a], Krassimir P. Velikov [b,c], Paul Venema [a,*], Erik van der Linden [a]

[a] Physics and Physical Chemistry of Foods, Department of Agrotechnology and Food Sciences, Wageningen University, P.O. Box 17, 6700 AA Wageningen, the Netherlands
[b] Unilever R&D Vlaardingen, Olivier van Noortlaan 120, 3133 AT Vlaardingen, the Netherlands
[c] Soft Condensed Matter, Debye Institute for NanoMaterials Science, Utrecht University, Princetonplein 5, 3584 CC Utrecht, the Netherlands

ARTICLE INFO

Article history:
Received 4 June 2018
Received in revised form 22 November 2018
Accepted 22 November 2018
Available online 24 November 2018

Keywords:
Whey protein isolate
Bacterial cellulose microfibrils
Mixed gel

ABSTRACT

Whey proteins can form different gel structures ranging from fine-stranded to particulate when appropriate conditions are applied. By incorporating polysaccharides, the gelation of WPI can be influenced. We investigated the heat-induced gelation of whey protein isolate (WPI) in the presence of bacterial cellulose (BC) microfibrils at pH 7 at different concentrations of NaCl. Our results showed that WPI and BC microfibrils form a homogeneous dispersion at pH 7. Upon heating, the WPI gel was formed independently in the presence of the BC microfibril gel, resulting in the formation of a composite gel. The gel structure and gelation dynamics of WPI was not influenced by the presence of BC microfibrils. However, the presence of BC microfibrils increased the storage modulus of the WPI gel, with an increase being negligible when the strength of the WPI gel is above a certain value. With an increase of NaCl concentration, the WPI gel structure changes from fine-stranded to a particulate gel, while the BC microfibril gel structure remains unchanged. No macroscopic phase separation could be observed in the WPI-BC microfibril gels. Our results showed that the rheological properties and water holding capacity of the WPI-BC microfibril mixed gels are mainly dominated by the WPI.

1. Introduction

Proteins and polysaccharides are common structuring components in foods. They are often present together due to their different functionalities like providing nutrition, gelling, thickening and stabilizing foods. The functionalities are dependent on the protein-polysaccharide interactions, which vary as a function of concentration, pH, temperature and ionic strength. Interactions between proteins and polysaccharides have been studied and reviewed extensively in literature [1–13]. When mixing a protein with a polysaccharide, there might be co-solubility, incompatibility or complex formation. Incompatibility is often observed as macroscopic phase separation [1,6,7,9,10,12].

A common food protein is whey protein which has received much interest in literature due to its various well-known functional and nutritional properties [14]. In particular, gelation, an important functional property of whey proteins, has received extensive attention. WPI has the ability to form different gel structures ranging from fine-stranded to particulate, under appropriate conditions [15]. By incorporating polysaccharides, the gelation of WPI can be influenced, allowing to tune structure of the gel. This also leads to a wide range of opportunities for designing novel structures and various functionalities for specific applications. In view of protein-polysaccharide mixtures, many polysaccharides have been added to WPI to influence the microstructures and the functionalities. Examples are xanthan [16–18], pectin [19], κ-carrageenan [20], carboxymethyl cellulose [21], galactomannan [22], and konjac glucomannan [23,24].

As one of the most abundant polysaccharides in nature, i.e. cellulose, cellulose microfibrils have gained attention as a key source for sustainable and natural materials [25]. In particular, microfibrils from bacterial cellulose (BC), has received increased attention in food fields due to its multi-functional potential uses, such as a thickening, gelling, emulsifying, stabilizing, texturizer and water-binding agent [26–32]. BC already finds its presence in food, such as the well-known dessert in the Philippines, named Nata de Coco [33], which has gained increasing popularity worldwide [26]. BC is a dietary fibre and therefore is interesting to be used in products from a health point of view, and it can be used as a structuring agent [34–36]. The BC microfibrils are of high purity compared to that of plant cellulose and contain only hydroxyl groups as functional groups [37]. The microfibrils in BC have a ribbon-like structure, having a width in the order of nanometers and a length in the order of micrometres. The microfibrils tend to agglomerate into space-filling networks in water, leading to a gel-like structure. Recently, colloidal dispersions of BC microfibrils were prepared from commercial nata de coco through an high-energy deagglomeration process [38]. Moreover, addition of carboxymethyl cellulose (CMC) in the BC microfibril

* Corresponding author.
E-mail address: paul.venema@wur.nl (P. Venema).

https://doi.org/10.1016/j.ijbiomac.2018.11.210
0141-8130/

dispersions during high-energy de-agglomeration treatment was reported to be able to form a more homogeneous dispersion, presumably due to the adsorption of CMC on the surface of BC microfibrils [39,40].

Despite numerous studies in literature on cellulose and BC microfibrils [37,41,42] and its broad potential applications in foods [43], only limited amount of research have focused on the interaction between WPI and BC microfibrils. In the current study, we investigated heat-induced biopolymer gels prepared from WPI and BC microfibrils at pH 7, at different NaCl concentrations. The rheological properties of the resulting gels were studied under small and large deformation, and the microstructure and water holding capacity were characterized, as a function of composition of the composite gel and its preparation.

2. Materials and methods

2.1. Preparation of whey protein isolate (WPI) solution

A 25 wt% WPI stock solution was prepared by dissolving the WPI (Bipro, Davisco, lot # JE 198-1-420, USA) powder in MilliQ water. The protein content of the WPI is 97.5% on a dry basis and 92.7% per 100 g powder. The mineral content per 100 g powder is: 750 mg sodium, 60 mg potassium, 130 mg calcium, 75 mg phosphorus and 25 mg magnesium. The concentration of WPI used throughout the study is the concentration of the WPI powder used for preparation. The solution was stirred at 4 °C for two days to ensure complete hydration. The pH of the WPI stock solution was adjusted to pH 7 using a 3 M NaOH solution. To remove undissolved protein, the solution was filtered using a syringe filter (Hydrophilic PES 0.45 μm, Millipore Millex-HP). An UV spectrophotometer (Cary 50 Bio, Varian) was used to determine the protein concentration of the solution at a wavelength of 280 nm, and a calibration curve determined from WPI solutions at known concentrations. We determine the WPI concentration of the final stock solution by diluting to concentrations low enough to allow for UV absorbance measurements. The stock solution was stored at 4 °C in the fridge for further use.

2.2. Preparation of bacterial cellulose (BC) microfibril dispersion

The dispersion of BC microfibrils was kindly provided by Unilever R&D Vlaardingen, the Netherlands. Details of the preparation procedure were described previously [38,39]. In short, the BC microfibrils were extracted from a commercially available source, Nata de Coco (Kara Santan Pertama, Indonesia) which consists of cubes of BC in syrup. Here several washing steps were applied to remove the flavours and colorants. Finally, the BC microfibrils were mechanically disrupted by passing them once through a Microfluidizer (M110S, Microfluidics) at a pressure of 1200 bar. The concentration of the stock dispersion used for sample preparation is 1 wt%.

2.3. Preparation of WPI-BC microfibril gels

The 25 wt% WPI stock solution and 1 wt% BC microfibril dispersion were used to prepare the mixtures. The mixtures were prepared by adding BC microfibrils to the WPI solution using a plastic pipette with a cut-off tip. All mixtures had the same final WPI concentration of 13 wt% and the BC concentrations varied from 0, 0.05, 0.1, 0.2, and 0.3 to 0.4 wt%. The pH of the mixtures was adjusted to pH 7 using a 3 M NaOH solution. The mixtures were stirred for 30 min to ensure a homogeneous mixing. Subsequently, the mixtures were heated in a water bath (Haake Phoenix II C25P) for gel preparation. The heating procedure consisted of first increasing temperature from 20 to 80 °C within 30 min (heating rate of 2 °C/min), holding at 80 °C for 30 min and then cooling from 80 to 20 °C within 30 min. The gels were stored at room temperature (20 °C) for further analysis.

Mixtures containing 13 wt% WPI and 0, 0.1 or 0.3 wt% BC microfibrils, were chosen to study the effect of NaCl on the gels. The NaCl solution was added after mixing WPI and BC microfibrils together. The final NaCl concentrations in the mixtures were 20, 50, 100, 200 and 250 mM, adjusted by using a stock NaCl solution of 3 M. All samples were mildly stirred for at least 30 min to provide homogeneous samples. The procedure for gel preparation is the same as described above.

2.4. Differential scanning calorimetry (DSC)

Prior to the measurement, about 50 mg sample was weighted in a sealed stainless-steel pan. Subsequently, the samples placed in the pan were transferred into the equipment (Diamond series DSC, Perkin Elmer, Pyris, USA). Measurements started with an equilibration at 20 °C for 2 min. The samples were then heated from 20 °C to 100 °C at a heating rate of 10 °C/min, held at 100 °C for 1 min, and cooled from 100 °C to 20 °C at a cooling rate of 10 °C/min. A second heating step from 20 °C to 100 °C at a heating rate of 10 °C/min was applied after an equilibration at 20 °C for 2 min. Measurements were performed in duplicate. We used the software of Pyris (Perkin Elmer) for data analysis.

2.5. Small deformation rheology

Small deformation rheological properties of the WPI-BC microfibril mixtures during gel formation were monitored on a stress-controlled rheometer (MCR 302, Anton Paar) using a sandblasted concentric cylinder geometry (CC17/TI/S-SN38492). Sample transfer to the rheometer was performed using a plastic pipette with a cut-off tip to minimize the BC microfibril alignment. A solvent trap was used and the sample was covered with a thin layer of paraffin oil to prevent evaporation. Storage modulus G′ and loss modulus G″ were measured at a frequency of 1 Hz and a strain of 0.1% during gel formation by increasing temperature from 20 to 80 °C at a heating rate of 2 °C/min, holding temperature at 80 °C for 30 min, cooling from 80 to 20 °C at a cooling rate of 2 °C/min and then holding the temperature at 20 °C for 30 min. Subsequently, a frequency sweep was carried out at a strain of 0.1% and the frequency being increased from 0.01 to 100 Hz within 30 min at 20 °C. In addition, a strain sweep at a frequency of 1 Hz was performed by increasing the strain from 0.01 to 1000% within 30 min at 20 °C to determine the linear visco-elastic region. The ratio of G″/G′ is indicated as tangent δ. In rheology measurement, at least duplicates were made for samples of 13 wt% WPI, 13 wt% WPI + 0.4 wt% BC, 13 wt% WPI + 0.3 wt% BC + 250 mM NaCl in order to check the consistency. The typical error is about 3% to 11%.

2.6. Scanning electron microscopy (SEM)

Gels for SEM analysis were prepared in 20 ml syringes (BD plastipak, Spain) following the same heating procedure as described above. Each of the WPI-BC mirofibril gels was cut into 5 pieces of 1 cm in diameter and 1.3 cm in height and then, these gel pieces were placed in 2.5% (v/v) glutaraldehyde solution for 8 h to crosslink the proteins. After crosslinking, the excess glutaraldehyde was removed by placing the gel pieces in MilliQ water while stirring overnight. The water was replaced gradually by acetone in 5 steps: starting from 10, 30, 50, and, 70 to 100% acetone. During each step, the samples were stirred for 1 h. The samples were then left in 100% acetone. Subsequently, the sample pieces were dried by critical point drying (CPD 300, Leica, Vienna, Austria). After drying, the samples were fractured and attached to a SEM sample holder using Carbon Conductive Cement (Leit-C, Neubauer Chemicalien, Germany). In order to remove all the solvent from the adhesive, the samples were stored overnight under vacuum. After sputter coating with a 10 nm thick layer of iridium (SCD 500, Leica, Vienna, Austria) the fractured surfaces were analyzed at 2 kV in a field emission scanning electron microscope (Magellan 400, FEI, Eindhoven, the Netherlands).

2.7. Confocal laser scanning microscopy (CLSM)

5 μl of 0.2% Rhodamine B and 10 μl of 0.05% Calcofluor White were added to stain the WPI [44] and BC [45], respectively, in a total sample volume of 1 ml. After adding the dye, the sample was mixed for 10 s on a vortex. 125 μl of the sample was transferred into CLSM cuvettes (Gene Frame 125 μl, Thermo Scientific), after which were sealed with a cover glass (Menzel-glaser, Thermo Scientific, Germany). For gel formation, the samples were heated in a water bath (Haake Phoenix II C25P) with the temperature increasing from 20 to 80 °C within 30 min, holding at 80 °C for 30 min and decreasing from 80 to 20 °C within 30 min. The samples were kept at room temperature for one day prior to image analysis. CLSM images were taken using a Zeiss LSM 510 META microscope (Zeiss, Germany) equipped with an Axiovert 200 M inverted microscope. The oil immersion objective (Plan-Apochromat 63x/1.4 oil DIC) was used. The excitation and emission wavelength of Rhodamine B are 543 nm and 560 nm. The excitation and emission wavelength of Calcofluor White are 405 nm and 420 nm.

2.8. Large deformation rheology

Gels were prepared in pre-lubricated (paraffin oil) 20 ml syringes (BD plastipak, Spain) and cut into cylinders of 20 mm in height and 20 mm in diameter using a wire cutter. To measure their fracture properties, an uniaxial compression test was performed using a Texture Analyser (TA-XT plus, Stable Micro Systems ltd., Godalming U.K) mounted with a 50 kg load cell and a cylindrical plastic probe of 75 mm in diameter. Paraffin oil was applied on both the top and bottom of the gel to prevent friction during compression. The gels were compressed to 80% of their initial height between two parallel plates at a constant deformation rate of 1 mm/s and a post-test speed of 10 mm/s. Each sample was measured four times at room temperature. We calculated the true stress, true strain and Young's modulus as described elsewhere [46].

2.9. Water holding capacity (WHC)

For the WHC measurement of the gels, we used a method described previously [46]. A microcentrifuge filtration unit containing an inner spin tube and a 2 ml Eppendorf tube (Axygen Biosciences, Inc., Union City, USA) was used. The gels were cut into cylinders of 10 mm in height and 4.8 mm in diameter using a cork borer and placed carefully at the bottom of the spin tube. Two pieces of filter paper (Macherey-Nagel MN 85/70 BF, 100 mm, Germany) with a diameter of 5 mm were placed on the spin tube to reduce grid size and avoid the leakage of the gels in the supernatant. Samples were centrifuged at 3350*g* for 15 min at 20 °C. The measurements were performed in duplicate. The water removed from the gel was collected at the bottom of the Eppendorf tube. The WHC of the gels is calculated as the remaining water (%) in the gel after centrifugation according to:

$$WHC = \frac{W_t - (W_g + W_{fp})}{W_t} * 100(\%) \quad (1)$$

where *WHC* is the water holding capacity (%), W_t is the amount of water present in the sample (g), W_g is the removed water from the sample at a given centrifugal force (g). W_{fp} is the water entrapped in the filter papers.

3. Results and discussion

3.1. Macroscopic images

The images of the WPI-BC microfibril mixtures both before and after gel formation (Fig. 1) showed that all samples were macroscopically a one phase system, and that the addition of BC microfibrils increased the turbidity of the mixture. Previous studies reported that dispersion of BC microfibrils prepared by high-energy mechanical deagglomeration showed a highly heterogeneous network consisting of fibril bundles, flocs, and voids (from ten to hundreds of micrometres)

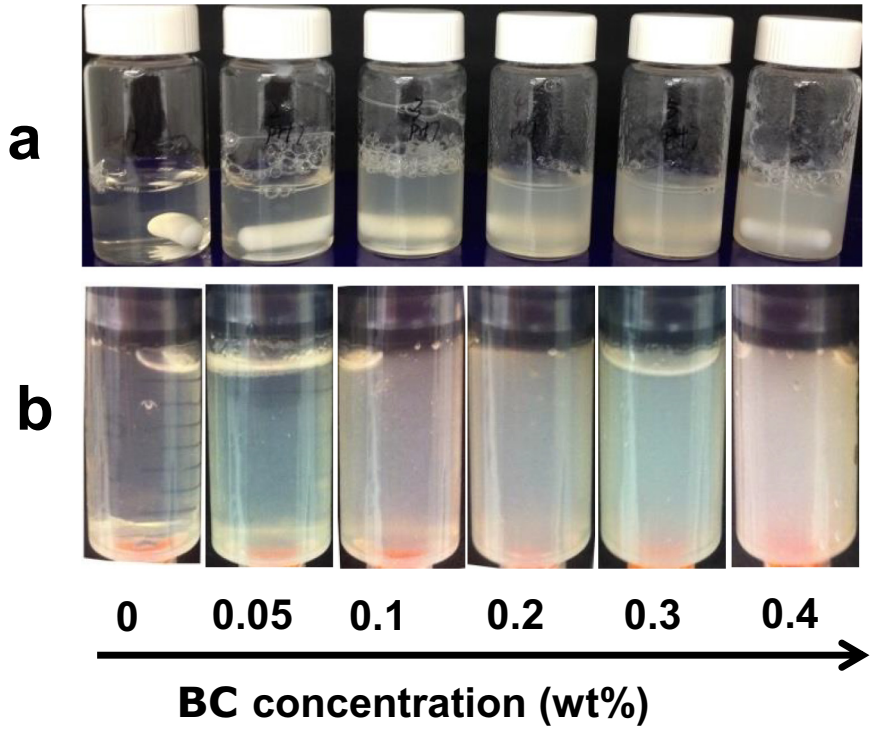

Fig. 1. Images of WPI-BC microfibril mixtures (a) and their corresponding heat-induced gels (b) at pH 7, prepared from 13 wt% WPI and BC microfibrils with concentrations of 0, 0.05, 0.1, 0.2, 0.3 or 0.4 wt%. The concentration of BC microfibrils (wt%) is indicated below each image.

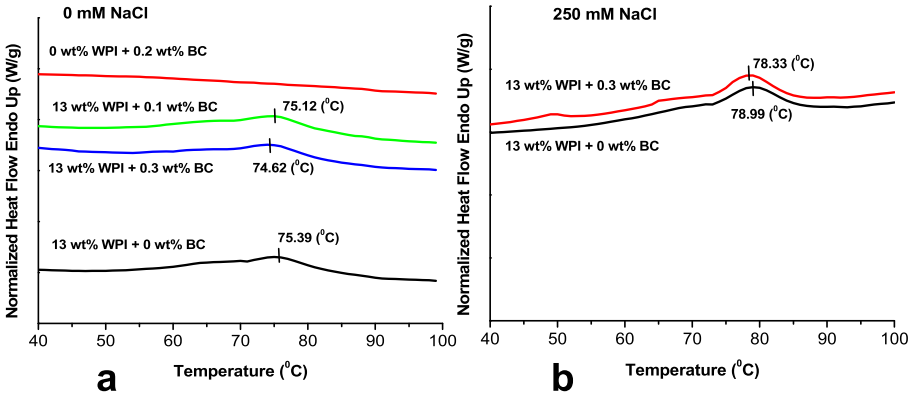

Fig. 2. DSC thermograms for pure WPI, pure BC microfibrils and the mixed WPI-BC microfibrils at NaCl concentrations of 0 (a) and 250 mM (b). The concentration of the samples is indicated in the Fig.

induced by their attractive interactions [38]. For BC microfibril dispersions, the minimal gel concentration was found to be 0.01 wt% at 1 cm sample height [38]. The formation of a gel by BC microfibrils was also confirmed by rheology [38]. Increasing the BC microfibril concentration was reported to lead to an increase in size of the flocs and decrease of the size of voids, however, the size of the bundles remained constant [38].

3.2. Differential scanning calorimetry (DSC)

DSC was used to determine the denaturation temperature change of the WPI-BC microfibril mixtures in comparison to that of the pure WPI.

For pure BC microfibrils, no distinct endothermic peaks were observed at pH 7 (Fig. 2a), confirming that BC is stable upon heating up to 100 °C [47]. For pure WPI, the endothermic peak around 75 °C is in accordance with the denaturation temperature of WPI found in literature [48]. In the mixture of WPI and BC microfibrils at concentrations of 0.1 and 0.3 wt%, the endothermic peak was similar to that of the pure WPI sample. The denaturation temperature was also not influenced by the presence of BC microfibrils. This is further shown in samples with NaCl concentration of 250 mM (Fig. 2b), where the mixture showed a similar endotherm peak to that of pure WPI sample. The increase in denaturation temperature of WPI at 250 mM NaCl is in agreement with literature [49]. As BC microfibrils do not show any endothermic peak during heating, and the denaturation temperature of the WPI-BC microfibril mixtures is independent of BC microfibril concentration, no specific interactions exist between WPI and BC microfibrils. This is in accordance with earlier findings by others [50].

3.3. Rheological properties

The results of the rheological experiments are shown below.

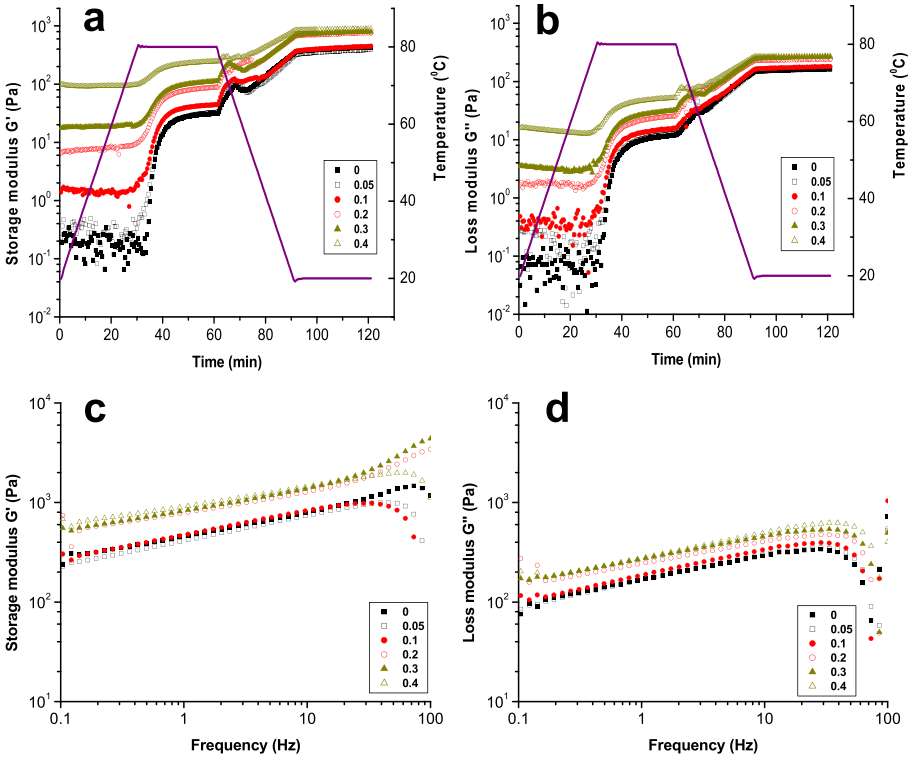

Fig. 3. Rheological properties of WPI-BC microfibril gels containing a constant 13 wt% WPI and BC microfibril concentrations at 0, 0.05, 0.1, 0.2, 0.3, and 0.4 wt%. The development of storage modulus G′ and the loss modulus G″ as a function of time during gel formation are shown in (a) and (b). The temperature profile is indicated by the purple line. Fig. (c) and (d) concerns a frequency sweep on the final gels and show the storage modulus G′ and loss modulus G″ as a function of frequency at the strain of 0.1%.

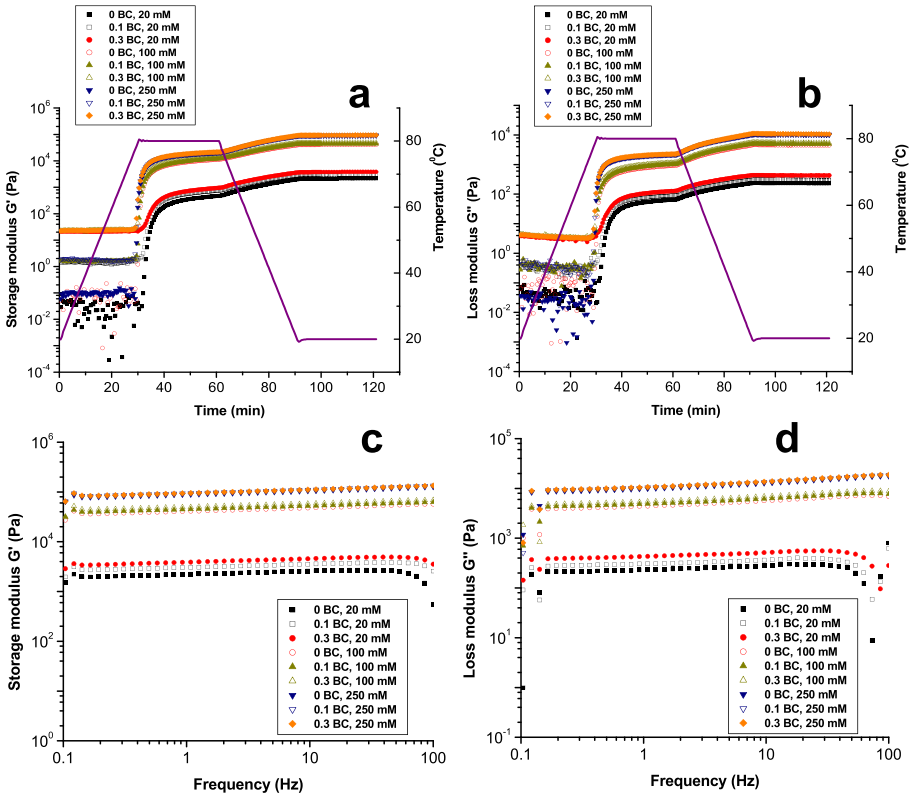

Fig. 4. Rheological properties of 13 wt% WPI gel containing 0, 0.1 and 0.3 wt% BC microfibrils with NaCl concentrations of 20, 100, and 250 mM. The storage modulus G′ (a) and loss modulus G″ (b) during gel formation are plotted as a function of time at a strain of 0.1% and frequency of 1 Hz. The purple line represents the temperature profile. Fig. (c) and (d) show the storage modulus G′ (c) and loss modulus G″ (d) of the gels as a function of frequency at strain of 0.1% at 20 °C.

Fig. 3 summarises the findings on the rheological properties of the WPI-BC microfibril gels. The G′ and G″ of the unheated samples are depicted at time = 0. Here one observes the effect of the BC microfibrillar dispersion since the proteins are not gelled yet. The BC microfibrillar dispersion indeed has a G′ larger than G″. The storage modulus G′ and loss modulus G″ of WPI-BC microfibril gels as a function of BC microfibril concentration (Fig. 3a and b) showed a comparable trend to that for the pure WPI. Both G′ and G″ of the samples increased upon heating at 80 °C and reached a plateau with time. Upon cooling from 80 to 20 °C, the G′ and G″ of gels with BC microfibrils showed an abrupt decrease, followed by a further increase of the G′ and G″ upon further cooling. The abrupt decrease in G′ and G″ is possibly caused by the creep of the paraffin oil between the gel surface and rheometer cup [51]. When holding at 20 °C, the G′ and G″ of all samples remained constant. The G″ development of all samples showed a similar trend to that of the G′ development (Fig. 3b). Plotting the G′ and G″ value as a function of BC microfibril concentration in WPI gels (Appendix 1), we observed a gradual increase of G′, reaching approximately 2 times higher (0.4 wt% BC) than the WPI sample without BC microfibrils. This implies that the addition of BC microfibrils to WPI resulted in higher firmness of the gel. In contrast to G′, the increase of G″ with increasing BC microfibril concentration is only a small effect for concentrations above 0.1 wt% BC microfibril. The G′ and G″ of all WPI gels with BC microfibrils showed the same linear dependency on frequency as that of the pure WPI gel (Fig. 3c and d), giving the same slope of the curve. The above findings suggest that the WPI gel dominates the rheological properties in the WPI-BC microfibril gels.

The pure WPI gels show a linear viscoelastic region (LVR) up to a strain of 10% (Appendix 2). With addition of 0.4 wt% BC, the LVR of the gels decreased to approximately 1% strain, suggesting gel breakdown at lower strain. In other words, the gels become more brittle

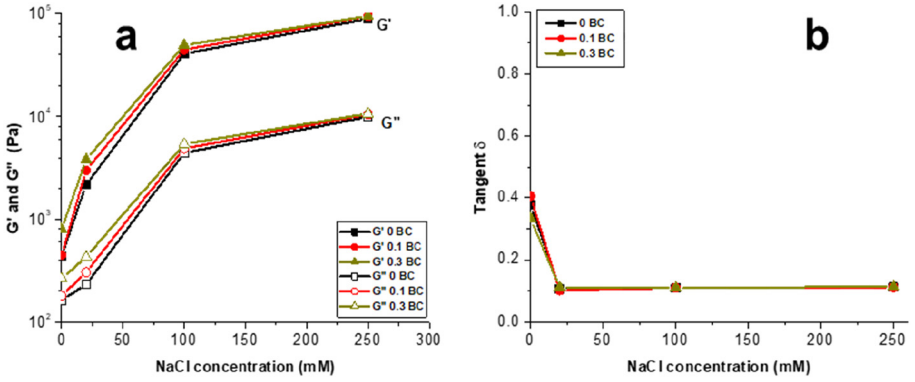

Fig. 5. Storage modulus G′ (filled symbols) and loss modulus G″ (open symbols) (a) and Tangent δ (b) as a function of NaCl concentration for 13 wt% WPI gels containing BC microfibril concentration of 0, 0.1, and 0.3 wt%. The values of G′ and G″ were taken from the last point of holding samples at 20 °C for 30 min after gel formation. Lines are used to guide the eye.

when BC microfibrils are added to the WPI gel. This graph shows that the strains applied (0.1%) in the different rheological tests are all in the linear regime for all BC concentrations.

At low ionic strength, WPI forms a fine-stranded gel structure upon heating. Increasing the ionic strength in the WPI solutions results in the formation of a more particulate gel structure [52,53]. To investigate the effect of NaCl concentration on heat-induced WPI-BC microfibril gelation, 20, 100 and 250 mM NaCl were added to the WPI-BC microfibril mixtures prior to heating. The rheological properties are shown below in Fig. 4.

The G′ (Fig. 4a) and G″ (Fig. 4b) as a function of time for WPI-BC microfibril gels with 20 mM NaCl are comparable to that of pure WPI with 20 mM NaCl. The G′ and G″ showed a sharp increase when temperature reaches 80 °C, followed by further increase upon cooling and holding temperature at 20 °C. Increasing NaCl to 100 mM, we observed a sharper increase in G′ and G″ upon temperature increasing to 80 °C supposedly

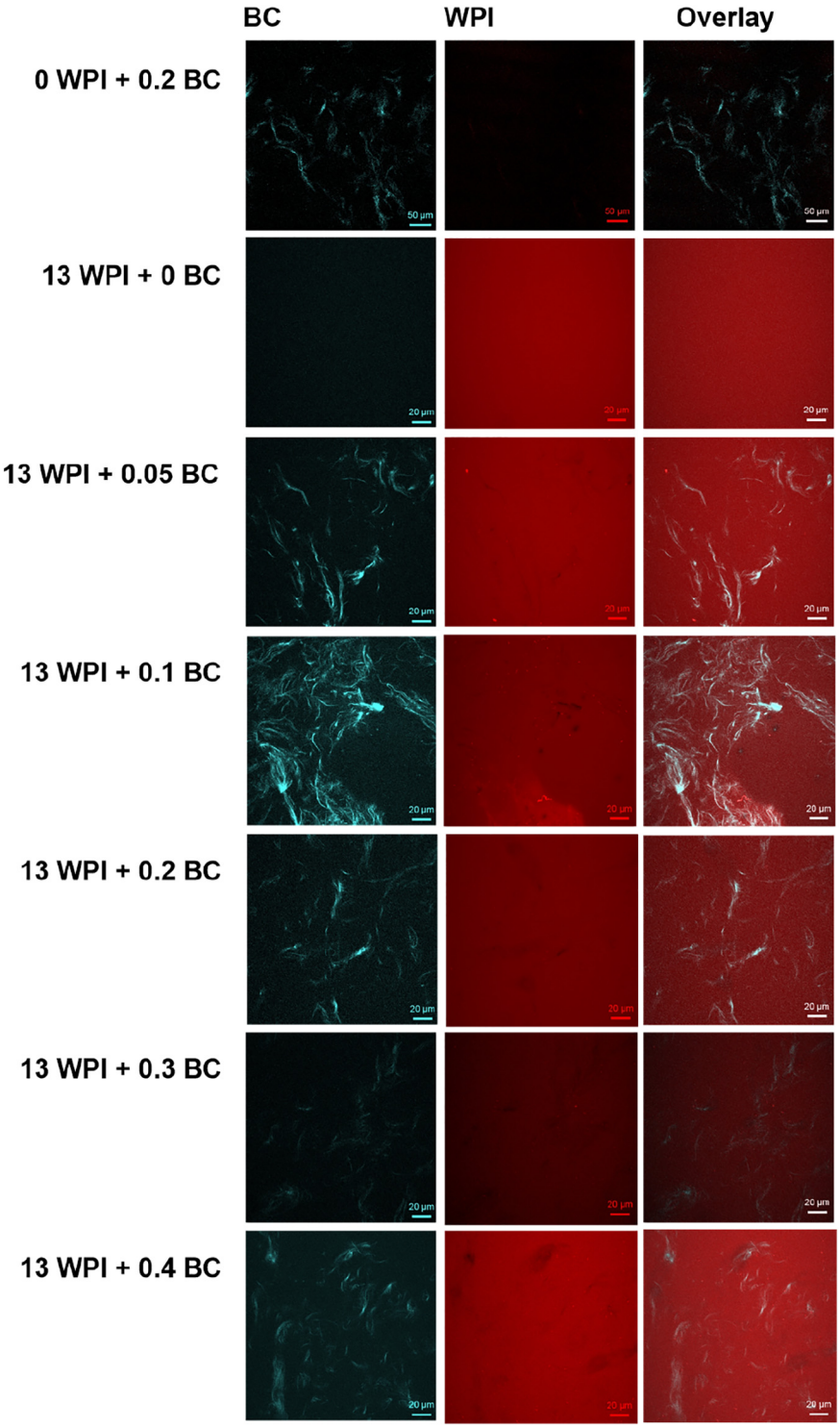

Fig. 6. CLSM images of WPI-BC microfibril gels containing 13 wt% WPI and BC microfibril concentrations of 0, 0.05, 0.1, 0.2, 0.3 and 0.4 wt%. The concentrations (wt%) are indicated next to the images. For each sample, images from the BC microfibril channel, WPI channel and the overlay image were shown. WPI is shown in red and BC microfibril in turquoise. The scale bar corresponds to 20 μm.

due to the accelerated aggregation caused by the screened intermolecular repulsion by NaCl. Upon further increase in NaCl concentration to 250 mM, the increase of G′ and G″ was comparable to the samples with 100 mM NaCl. We conclude that the addition of 100 mM NaCl leads to a stronger gel. Higher NaCl concentrations do not lead to a further gel strengthening. Comparing Fig. 3c and d and Fig. 4c and d yields that the G′ shows a stronger frequency dependence at zero salt concentration than at 100 mM NaCl. Plotting the G′ and G″ values as a function of NaCl concentration as shown in Fig. 5a, one can observe that the increase of G′ and G″ is mainly dominated by NaCl concentration, the concentration of BC microfibrils showed only a small effect on G′ and G″. In addition, the tangent δ (Fig. 5b) of the WPI-BC microfibril gels showed a comparable trend and value to that of pure WPI gels upon increasing NaCl concentration, suggesting that the WPI gel structure in the WPI-BC microfibril gel is structured in the same way as the pure WPI gel [54]. Interestingly, tangent δ decreased upon addition of NaCl concentration up to 25 mM, and remained constant afterwards. The G′ and G″ of all WPI-BC microfibril gels were independent of frequency as shown in Fig. 4c and d. The strain sweep (Appendix 3) showed that the linear visco-elastic regime of the WPI gel with 0.4 wt% BC microfibrils is the same as the pure WPI gel (at NaCl concentration of 250 mM). This graph shows that that the strains applied (0.1%) in the different rheological tests are all in the linear regime for all salt concentrations.

In Appendix 4, the gel storage modulus G′ and loss modulus G″ of pure WPI, pure BC microfibrils, and the WPI-BC microfibril mixtures at both 0 and 250 mM NaCl are presented. The G′ and G″ of 0.3 wt% pure BC microfibril dispersion remained constant upon heating and cooling, both at 0 and 250 mM. This again shows that BC does not gel upon heating (both at 0 and 250 mM NaCl), an observation in line with our DSC data and literature [28,29]. In the mixture containing 13 wt% WPI and 0.3 wt% BC microfibrils, the development curve of G′ and G″ during heating over time at both 0 and 250 mM was comparable to that of pure 13 wt% WPI gel. However, the value of the G′ and G″ in the mixture is higher than that of the pure WPI gel at 0 mM NaCl, indicating a synergistic effect upon addition of BC microfibrils. At 250 mM NaCl, the values of the G′ and G″ of the mixture are close to that of the pure WPI gel, suggesting that WPI gel dominates the rheological properties of the mixed gel and the synergistic effect caused by BC microfibrils was too small in comparison to the strength of the WPI gel. In addition, the G′ and G″ of BC microfibrils were independent of frequency at both 0 mM and 250 mM NaCl. The G′ and G″ of the WPI-BC microfibril gels at both 0 and 250 mM NaCl showed similar dependency on frequency as the pure WPI gels at the same WPI concentration, indicating that WPI gel is the dominant one in the mixture. We note that the G′ and G″ for the 0.3% BC unheated gels without WPI are slightly higher than 0.3% BC unheated gels with 13% WPI. This is possibly caused by WPI slightly weakening the BC network.

Since BC microfibrils are not exhibiting gelation upon heating, WPI is the only gelling agent during heating. Our results showed that adding high enough BC microfibril concentration leads to a firmer overall gel. This increase is not observed when NaCl is added. Instead, in that case the WPI-BC microfibril gels show the same rheological properties as the pure WPI gels. This is probably related to the fact that the increase of gel firmness resulted from NaCl is much larger than the increase of gel firmness resulted from BC microfibrils addition up to 0.4 wt%. Consequently, the change of G′ and G″ of the gels are dominated by NaCl concentration, resulting in stronger WPI gels. Our results on firmer WPI gels upon salt increase are in agreement with the literature [17].

In conclusion, we found that high enough BC microfibril concentration leads to increase in the firmness (synergistic effect) of the WPI gels. With the information provided this far, the reasons can be threefold. The amount of the solvent entrapped in the BC phase could be increased, thus, leading to the concentration of the protein phase, and increase of the gel firmness [55]. On the other hand, the BC network itself could lead to an increase in firmness by itself, and this could then add to the overall gel strength. A third option is both phenomena to be relevant for the increase.

3.4. Confocal laser scanning microscopy (CLSM)

To further investigate the WPI-BC microfibril gels at different BC microfibril and NaCl concentrations and possibly explain the synergy between WPI and BC microfirbils, we studied the microstructure of the gels using CLSM.

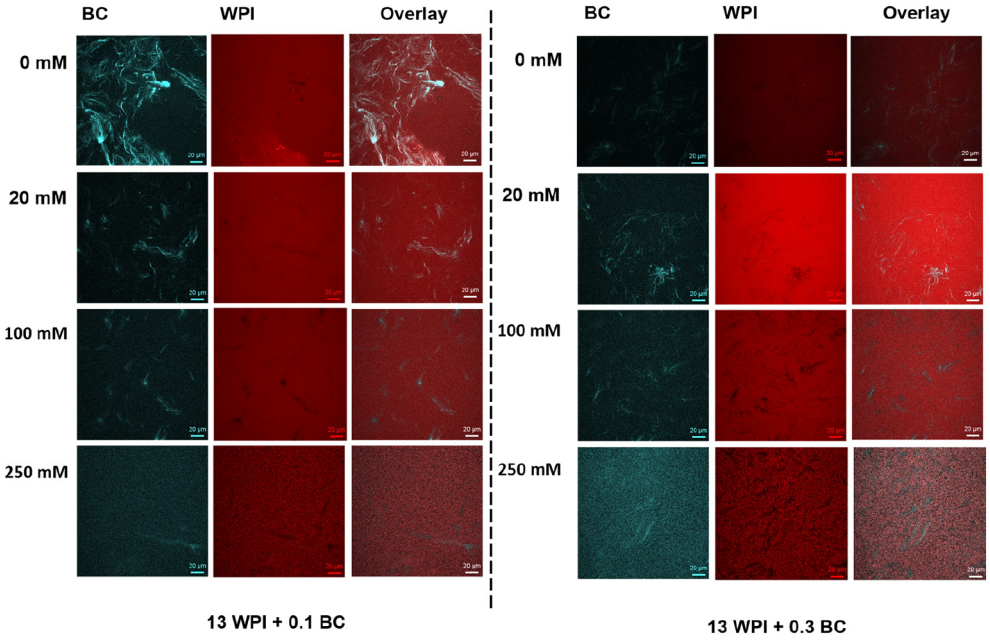

Fig. 7. CLSM images of WPI-BC microfibril gels with NaCl of 0, 20, 100 and 250 mM. The NaCl concentrations (mM) are indicated on the left side of the images. The WPI and BC concentrations (wt%) are indicated below the images. Images from the BC microfibril channel, WPI channel and the overlay image were shown. The BC microfibrils are shown in turquoise and the WPI is shown in red. The scale bar corresponds to 20 μm. The black dashed line in the middle of the Fig. separates the samples containing 13 wt% WPI and 0.1 wt% BC microfibrils from the samples containing 13 wt% WPI and 0.3 wt% BC microfibrils.

In Fig. 6, we observed a homogeneous WPI network in pure 13 wt% WPI gel. In WPI gels containing BC microfibrils, we also observed a homogeneous network for the WPI, independent of the concentration of BC microfibrils. In addition, we observed clusters of BC microfibrils distributed over the system. No macroscopic phase separation could be observed for the any of the BC microfibril concentrations. The distribution of these clusters of BC microfibrils and corresponding voids (ranging from tens to thousands of micrometres) varies depending on concentration of BC microfibrils, which has already been reported previously [38]. In the CLSM overlay images where both WPI and BC microfibril are shown, we observed that WPI forms a homogeneous gel network (on the length scale probed by CLSM), even when the BC microfibrils are present. This suggests that the presence of BC microfibrils does not influence the WPI gel network structure on the length scale of micrometre or larger. Similar results have also been reported in WPI gels with other protein [56] or polysaccharide [19] systems.

We observed (Fig. 7) that increasing the concentration of NaCl did not affect the distribution of BC microfibrils in the mixed gels, however, the WPI gels become coarser. The coarseness increased with increasing NaCl concentration. The amount of BC microfibrils (0.1 wt% or 0.3 wt%) did not influence the structure of the mixed gels significantly. Previous studies have shown that adding NaCl has a significant influence on the gelation of WPI, where the gel network becomes coarser by changing from a fine-stranded to a particulate gel [57,58]. BC microfibril gel structure was found to be unaffected by NaCl concentration, as observed in the CLSM images (Appendix 5). Adding different concentrations of NaCl to the WPI-BC microfibril gels showed that only the structure of the WPI gels was influenced, to an extent that is similar to that of the pure WPI gels.

3.5. Scanning electron microscopy (SEM)

SEM was used to determine the morphology of the WPI-BC microfibril gels at different BC microfibril and NaCl concentrations.

The pure WPI gel showed a smooth and homogeneous structure, as shown in Fig. 8a. Upon addition of BC microfibrils, we observed a homogeneous WPI gel with BC microfibrils distributing uniformly in the WPI gel. Increasing the BC microfibril concentration from 0.05 wt% to 0.4 wt% in WPI gels, the heterogeneity of the gel also increased [38]. To have a closer look at the morphology of the WPI gel with different

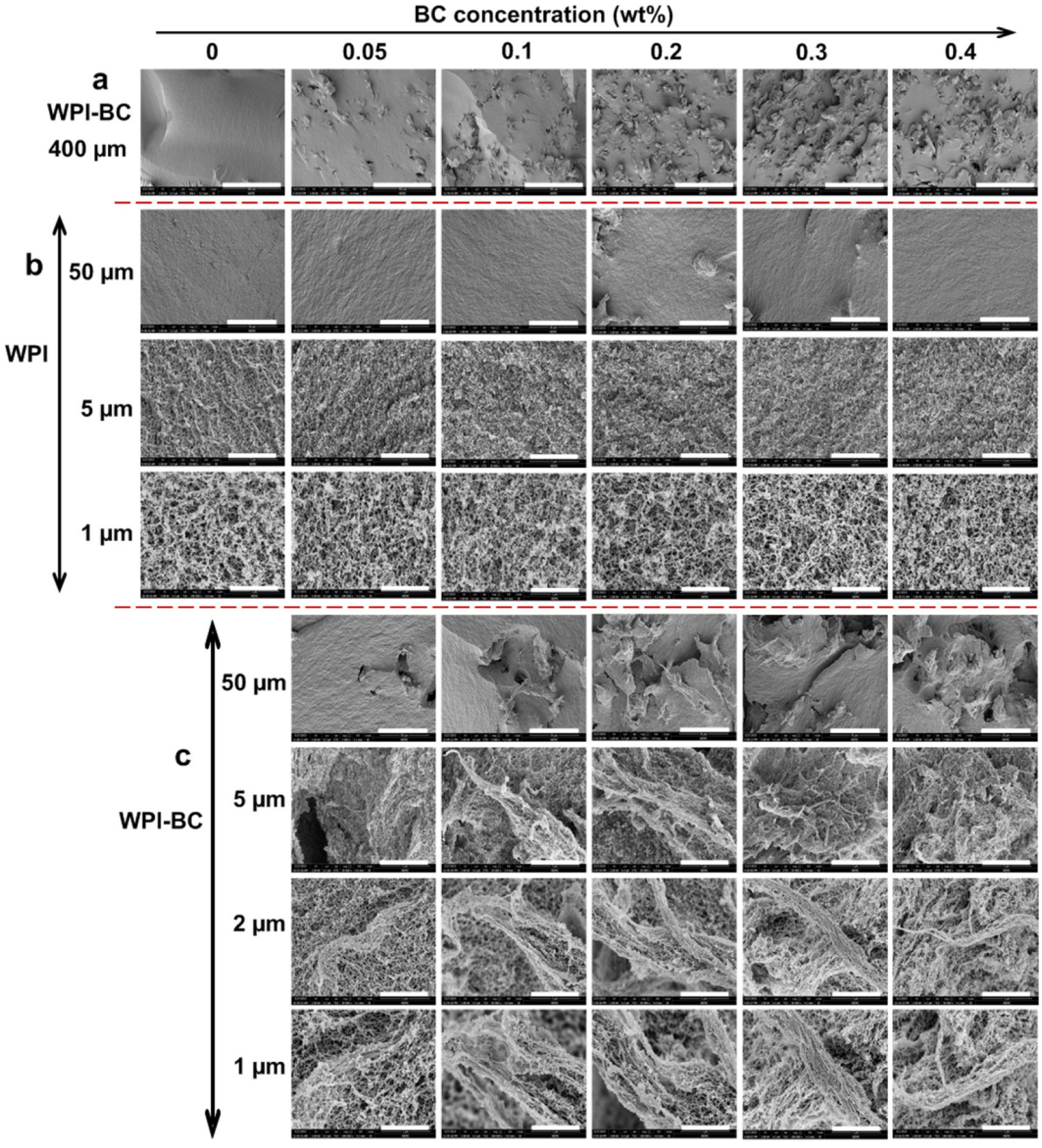

Fig. 8. SEM images of 13 wt% WPI containing 0, 0.05, 0.1, 0.2, 0.3 and 0.4 wt% BC microfibrils. The overall structure of the gels at low magnification is shown in (a). An area where mainly WPI is present is shown in (b). An area where both WPI and BC microfibrils are present is shown in (c). Scale bars correspond to 400 μm, 50 μm, 5 μm, 2 μm and 1 μm.

concentrations of BC microfibrils, we imaged the sample area where mainly WPI is present, as shown in Fig. 8b. The WPI gel structure formed in samples containing BC microfibrils were similar to the structure of a pure WPI gel, independent of BC microfibril concentration, suggesting that the presence of BC microfibrils did not significantly influence the WPI gel structure. When the area where both WPI and BC microfibrils are present was imaged, we observed BC microfibril bundles and the dimensions of the bundles vary. In addition, we also observed the growth of WPI protein structures along the BC microfibril bundles, presumably either covering the surface of the BC microfibril bundles or being close to the BC microfibril bundles. SEM images show that BC fibrils by themselves have a smooth surface while in the presence of WPI [59], as in Fig. 8, the fibrils are decorated by proteins. It is not clear whether this is due to specific adsorption of WPI on the BC microfibril surface or simply due to the fact that the WPI proteins are close to the BC bundles.

When 20 mM NaCl is added, the WPI-BC microfibril gels become translucent. Upon increasing NaCl concentration to 250 mM, the gels become increasingly opaque (Fig. 9a). An increase in coarseness of the WPI gel is also observed, as shown in Fig. 9b and c. Adding 0.1 or 0.3 wt% BC microfibrils did not show a significant difference on the macroscopic appearance of the gels. At higher magnification, we observed a gel structure changing from fine-stranded to particulate gel with increasing NaCl concentration (Fig. 9b and c). This is related to reduced electrostatic repulsion between proteins at higher NaCl concentration, facilitating the protein aggregation into a particulate gel structure [60]. The influence of BC microfibrils on the WPI gel structure with added NaCl was comparable to the gels without added NaCl. Interestingly, with increase in NaCl concentration, we observe more BC microfibril surface that seems to be not covered or hidden by protein (Fig. 9d). This may be due to the stronger aggregation of the proteins among themselves at larger NaCl concentration. The presence of BC microfibrils did not show a distinct influence on the structure of the composite gel. It can be concluded that the addition of NaCl in WPI-BC microfibril gels only influenced the protein aggregation, leading to a coarser protein gel, to a similar extent as to what is observed in pure WPI gels upon increasing NaCl concentration. This is in-line with the DSC results,

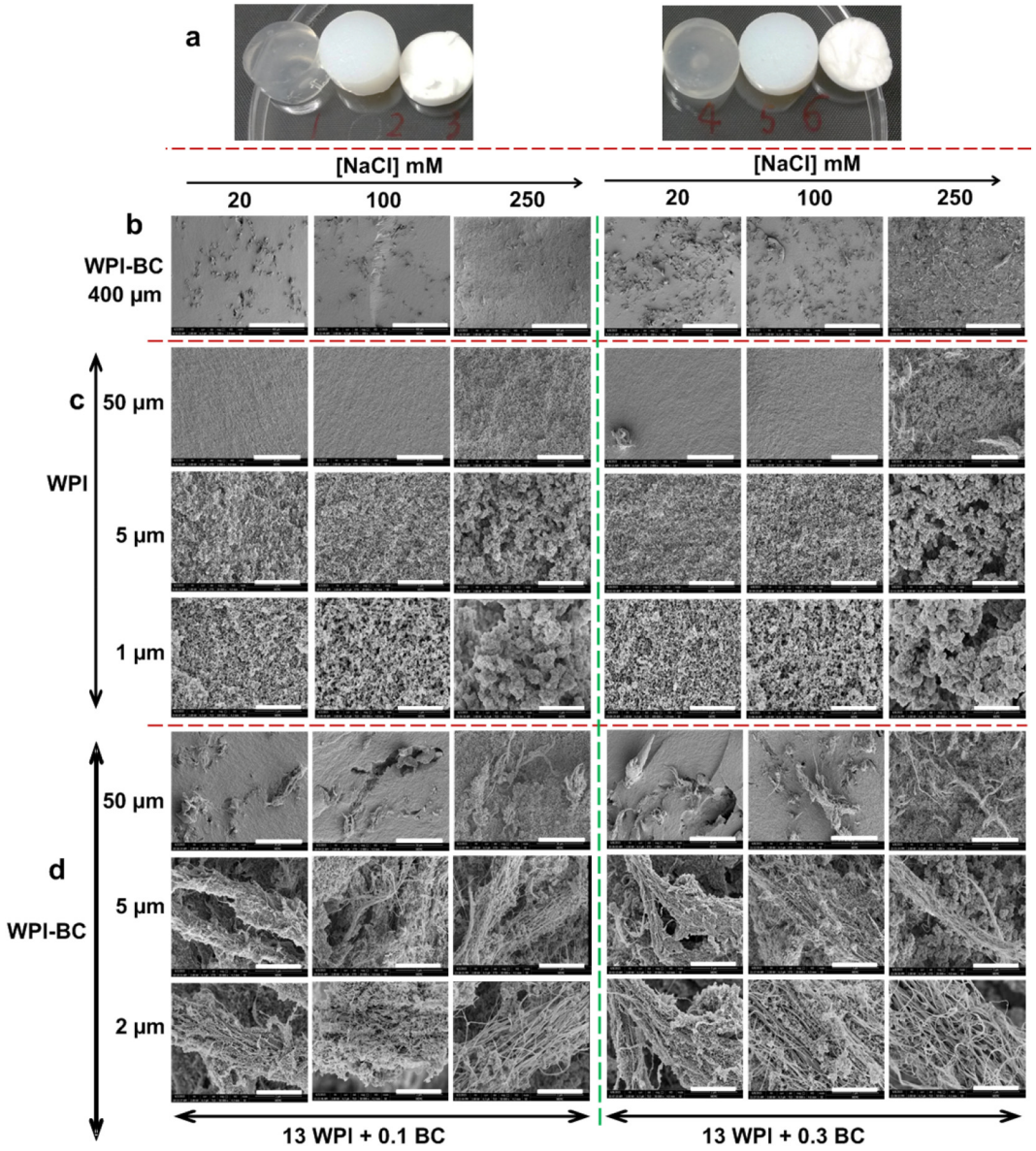

Fig. 9. SEM images of 13 wt% WPI containing 0, 0.1, and 0.3 wt% BC microfibrils at NaCl concentration of 20, 100, and 250 mM. The visual appearance of the gels is shown in (a). The overall structure of the gels at low magnification is shown in (b). An area where mainly WPI is present is shown in (c). An area where both WPI and BC microfibrils are present is shown in (d). The NaCl concentration (mM) is indicated on the top of the images. Scale bars correspond to 400 µm, 50 µm, 5 µm, 2 µm and 1 µm. The green dashed line in the middle of the Fig. separates the samples containing 13 wt% WPI and 0.1 wt% BC microfibrils from the samples containing 13 wt% WPI and 0.3 wt% BC microfibrils.

rheological properties, and CLSM images, where also no specific interactions between WPI and BC microfibrils could be concluded.

From the CLSM and SEM images, we can conclude that adding BC microfibrils did not influence the WPI gel structure. Overall, for any NaCl concentration, in mixed gels of WPI and BC microfibrils, the WPI forms a gel structure independent from the BC microfibril gel, and with a structure similar to that in a pure WPI gel.

3.6. Large deformation response

To investigate how BC microfibrils affect the breakdown properties of the WPI gels at different NaCl concentrations, large deformation rheology was performed. The macroscopic appearance of the gels is shown in Appendix 6 and the true stress and true strain of gels under uniaxial deformation are shown in Fig. 10. The Young's modulus and fracture stress as a function of BC microfibril concentration are shown in Appendix 7.

Both increasing BC microfibril and NaCl concentrations resulted in more opaque gels, as shown above (Appendix 6). For pure WPI gel without NaCl (Fig. 10A), the gel was very weak and did not fracture completely under compression. With addition of BC microfibrils, the gels became stiffer, but were still weak and fractured only partially (Fig. 10A). This is due to the high elastic properties of WPI gel. Adding BC microfibrils decrease the elasticity of the gels, in line with the small deformation rheological properties, but the gels were still not brittle enough to fracture completely. With addition of 50 mM NaCl, all the gels eventually fractured. Upon increase in NaCl concentration, the gels fractured at larger stress but lower strain, corresponding to a firmer but more brittle gel with a coarser gel structure [17,61]. We note that the fracture properties of WPI-BC microfibril gels with 100 mM NaCl are comparable to those of gels with 200 mM NaCl. This is related to the balance between formation of larger aggregates and less connectivity between the aggregates [62,63]. Overall, the fracture behaviour of the WPI gels with BC microfibrils under large deformation is comparable to that of the pure WPI gels, independent of BC microfibril concentration. The difference in fracture behaviour induced by the NaCl addition was attributed to WPI gel structural changes, as confirmed by CLSM and SEM images. In Appendix 7B, it also shows that the concentration of BC microfibrils in the WPI-BC mirofibril gel did not significantly alter the fracture stress of the gels in comparison to the pure WPI gels at the same concentration. This is due to the strong gel formed by WPI, which dominates the gel facture properties. Our results are in agreement with literature in that for mixed gels with two independent networks, the stronger gel of the two dominates the fracture behaviour [56].

Young's modulus was determined from the initial slope of the stress over strain curve (strain 0.01–0.1). As shown in Appendix 7A, the Young's modulus of the pure WPI gels increased significantly with increasing NaCl concentration, due to the formation of thicker protein strands. Upon BC microfibrils addition, the Young's modulus slightly increased with increasing BC microfibril concentration in the mixed gels, with the exception of the gels prepared at 200 mM NaCl where the Young's modulus is comparable to that of the pure WPI gels with 200 mM NaCl.

3.7. Water holding capacity (WHC)

Water holding capacity of the WPI-BC microfibril gels was determined at varying concentrations of BC microfibrils and NaCl (Fig. 11).

In WPI-BC microfibril gels without NaCl, the WHC increased slightly with increasing BC microfibril concentration. This is attributed to the good water binding ability of BC [26], which has also been reported in other studies [28,64,65]. Okiyama et al. [65] measured the water holding capacity of BC and found that as a filler, BC has the highest water holding capacity among commercial cellulose products. Because of its high water holding capacity, it was reported that BC can be used as a thickening agent for reducing energy content of food products [28] and fat replacement in foods [64]. Upon addition of NaCl, the WHC of the gels decreased with increase in NaCl concentration. At a NaCl concentration of 50 mM, the WHC gradually decreased with increasing BC concentration. At 100 mM NaCl, the decrease of the WHC is less pronounced with increase of BC microfibril concentration. When 200 mM NaCl is added, the WHC of the WPI-BC microfibril gels is comparable to that of the pure WPI gels. In line with literature, the WHC of pure WPI gels decreases with increasing NaCl concentration [17,61,63]. The decreased WHC of WPI gels due to addition of NaCl is related to a

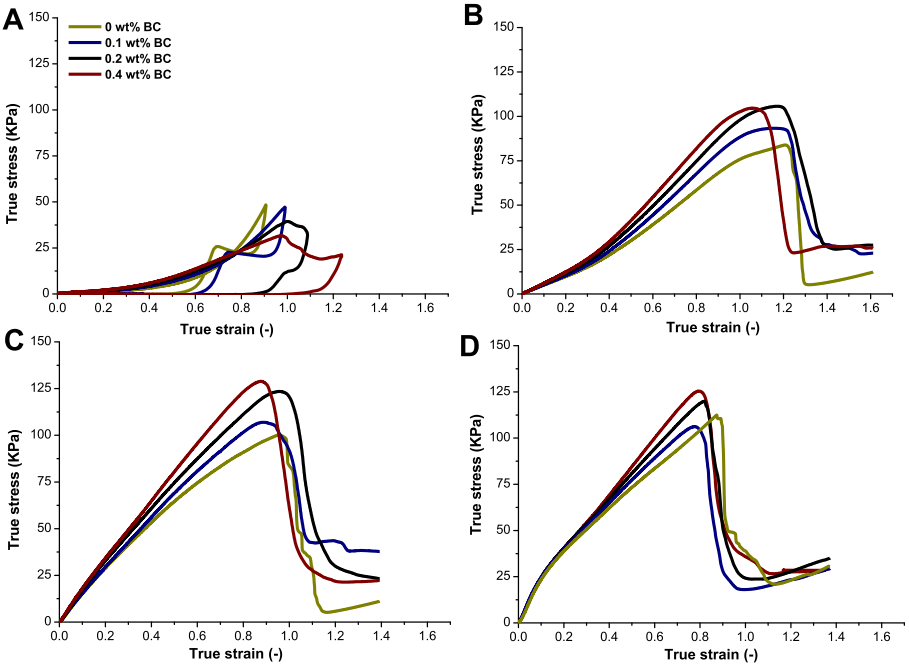

Fig. 10. The True stress (KPa) over true strain (-) of WPI-BC microfibril gels containing 13 wt% WPI and BC microfibrils of 0, 0.1, 0.2 and 0.4 wt%. The NaCl concentration in A, B, C, D corresponds to 0, 50, 100 and 200 mM.

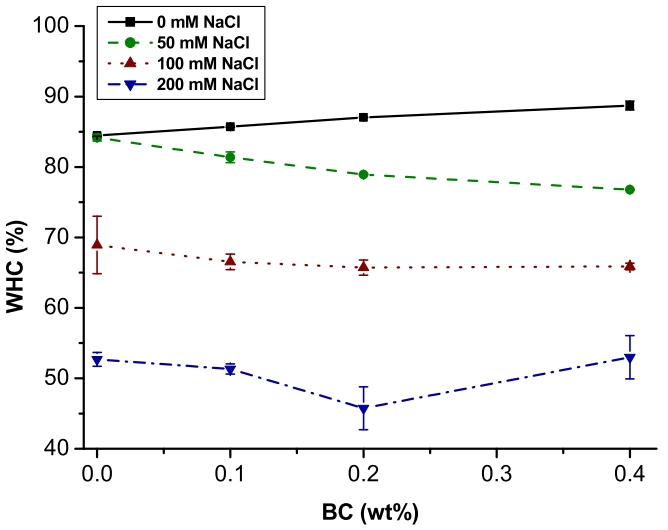

Fig. 11. WHC of WPI-BC microfibril mixed gels containing 13 wt% WPI and BC concentrations of 0, 0.1, 0.2 and 0.4 wt%. The NaCl concentrations in the mixed gels vary from 0, 50, and 100 to 200 mM.

coarser microstructure. Meanwhile, addition of NaCl was also found to decrease the WHC of BC mcirofibrils [47]. Expectedly, mixed gels of WPI and BC microfibrils exhibit a decrease of WHC upon addition of NaCl at 100 and 200 mM NaCl, the WHC is less influenced by the BC microfibrils; in fact the WHC of the mixed gels is comparable to that of the pure WPI. This is presumably due to the fact that the WHC of WPI is already rather low at higher salt concentrations due to the coarser structure. Previous results showed that the microstructure and stiffness of gels show a correlation to their WHC [46,63]. We accordingly plotted the Young's modulus as a function of WHC in Appendix 8.

For pure WPI gels, the Young's modulus showed a negative correlation with the WHC. With increasing NaCl concentration, the stiffness and coarseness of the gel increased, thereby facilitating the water removal. This result is in line with earlier work on WPI gels by Urbonaite et al. [63]. The addition of different concentrations of BC microfibrils to the WPI did not change the relation between the Young's modulus and WHC significantly. This again confirmed that the WHC of the WPI-BC microfibril gels is dominated by the properties of the WPI gel, i.e. the concentration of NaCl in this study.

4. Conclusions

We have shown that the WPI gel structure within a WPI-BC microfibril gel is independent of the presence of BC microfibrils. The gel consists of a WPI gel network and a BC microfibrillar network. In the mixed gels, NaCl only influences the WPI gel structure. At lower NaCl concentrations, the rheological properties of WPI gels can be altered by the addition of BC microfibrils. At higher NaCl concentration, the rheological properties are dominated by the (much stronger) WPI gel. The presence of BC microfibrils did not show a significant influence on the WPI gelation dynamics and gel structure. The concentration of BC microfibrils did not significantly influence the large deformation rheology nor the WHC of the WPI-BC microfibril mixed gels. Properties of the gels are dominated by the properties of the WPI gel. The ability of the BC microfibril gel to modify the WPI gel properties in the mixed gel is the largest for the weakest WPI gel structure and increases with increasing concentration of BC microfibrils.

Acknowledgement

This work is supported by NanoNextNL, a micro and nanotechnology consortium of the Government of the Netherlands and 130 partners. We thank Norbert de Ruijter for CLSM image analysis and Tiny Franssen-Verheijen for SEM image analysis. We thank Dr. A. Kijk and Dr. S. Veen for providing the dispersion of bacterial cellulose.

Appendix A. Supplementary data

Supplementary data to this article can be found online at https://doi.org/10.1016/j.ijbiomac.2018.11.210.

References

[1] J.-L. Doublier, C. Garnier, D. Renard, C. Sanchez, Protein–polysaccharide interactions, Curr. Opin. Colloid Interface Sci. 5 (3) (2000) 202–214.
[2] C.G. De Kruif, F. Weinbreck, R. de Vries, Complex coacervation of proteins and anionic polysaccharides, Curr. Opin. Colloid Interface Sci. 9 (5) (2004) 340–349.
[3] M. Corredig, N. Sharafbafi, E. Kristo, Polysaccharide–protein interactions in dairy matrices, control and design of structures, Food Hydrocoll. 25 (8) (2011) 1833–1841.
[4] E. Dickinson, Stability and rheological implications of electrostatic milk protein–polysaccharide interactions, Trends Food Sci. Technol. 9 (10) (1998) 347–354.
[5] S. Turgeon, M. Beaulieu, C. Schmitt, C. Sanchez, Protein–polysaccharide interactions: phase-ordering kinetics, thermodynamic and structural aspects, Curr. Opin. Colloid Interface Sci. 8 (4) (2003) 401–414.
[6] V. Tolstoguzov, Functional properties of food proteins and role of protein-polysaccharide interaction, Food Hydrocoll. 4 (6) (1991) 429–468.
[7] V.Y. Grinberg, V. Tolstoguzov, Thermodynamic incompatibility of proteins and polysaccharides in solutions, Food Hydrocoll. 11 (2) (1997) 145–158.
[8] J.M. Rodríguez Patino, A.M.R. Pilosof, Protein–polysaccharide interactions at fluid interfaces, Food Hydrocoll. 25 (8) (2011) 1925–1937.
[9] C. Schmitt, S.L. Turgeon, Protein/polysaccharide complexes and coacervates in food systems, Adv. Colloid Interf. Sci. 167 (1–2) (2011) 63–70.
[10] O.G. Jones, D.J. McClements, Recent progress in biopolymer nanoparticle and microparticle formation by heat-treating electrostatic protein–polysaccharide complexes, Adv. Colloid Interf. Sci. 167 (1–2) (2011) 49–62.
[11] Q. Ru, Y. Wang, J. Lee, Y. Ding, Q. Huang, Turbidity and rheological properties of bovine serum albumin/pectin coacervates: effect of salt concentration and initial protein/polysaccharide ratio, Carbohydr. Polym. 88 (3) (2012) 838–846.
[12] E. Bouyer, G. Mekhloufi, V. Rosilio, J.-L. Grossiord, F. Agnely, Proteins, polysaccharides, and their complexes used as stabilizers for emulsions: alternatives to synthetic surfactants in the pharmaceutical field? Int. J. Pharm. 436 (1) (2012) 359–378.
[13] T. Wagoner, B. Vardhanabhuti, E.A. Foegeding, Designing whey protein–polysaccharide particles for colloidal stability, Annu. Rev. Food Sci. Technol. 7 (2016) 93–116.
[14] J. De Wit, Nutritional and functional characteristics of whey proteins in food products, J. Dairy Sci. 81 (3) (1998) 597–608.
[15] J.M. Aguilera, Gelation of whey proteins: chemical and rheological changes during phase transition in food, Food Technol. 49 (10) (1995) 83–89.
[16] D. Zasypkin, E. Dumay, J. Cheftel, Pressure-and heat-induced gelation of mixed β-lactoglobulin/xanthan solutions, Food Hydrocoll. 10 (2) (1996) 203–211.
[17] S. Barbut, Effect of sodium level on the microstructure and texture of whey protein isolate gels, Food Res. Int. 28 (5) (1995) 437–443.
[18] C.M. Bryant, D.J. McClements, Influence of xanthan gum on physical characteristics of heat-denatured whey protein solutions and gels, Food Hydrocoll. 14 (4) (2000) 383–390.
[19] S.L. Turgeon, M. Beaulieu, Improvement and modification of whey protein gel texture using polysaccharides, Food Hydrocoll. 15 (4–6) (2001) 583–591.
[20] S. Mleko, E.C.Y. Li-Chan, S. Pikus, Interactions of κ-carrageenan with whey proteins in gels formed at different pH, Food Res. Int. 30 (6) (1997) 427–433.
[21] C. Capitani, O.E. Pérez, B. Pacheco, M. Teresa, A.M.R. Pilosof, Influence of complexing carboxymethylcellulose on the thermostability and gelation of α-lactalbumin and β-lactoglobulin, Food Hydrocoll. 21 (8) (2007) 1344–1354.
[22] C. Tavares, J.L. Da Silva, Rheology of galactomannan–whey protein mixed systems, Int. Dairy J. 13 (8) (2003) 699–706.
[23] J.T. Tobin, S.M. Fitzsimons, V. Chaurin, A.L. Kelly, M.A. Fenelon, Thermodynamic incompatibility between denatured whey protein and konjac glucomannan, Food Hydrocoll. 27 (1) (2012) 201–207.
[24] A.R. Abhyankar, D.M. Mulvihill, M.A. Fenelon, M.A.E. Auty, Microstructural characterization of β-lactoglobulin-konjac glucomannan systems: effect of NaCl concentration and heating conditions, Food Hydrocoll. 24 (1) (2010) 18–26.
[25] R.J. Moon, A. Martini, J. Nairn, J. Simonsen, J. Youngblood, Cellulose nanomaterials review: structure, properties and nanocomposites, Chem. Soc. Rev. 40 (7) (2011) 3941–3994.
[26] Z. Shi, Y. Zhang, G.O. Phillips, G. Yang, Utilization of bacterial cellulose in food, Food Hydrocoll. 35 (0) (2014) 539–545.
[27] A. Okiyama, M. Motoki, S. Yamanaka, Bacterial cellulose II. Processing of the gelatinous cellulose for food materials, Food Hydrocoll. 6 (5) (1992) 479–487.
[28] A. Okiyama, M. Motoki, S. Yamanaka, Bacterial cellulose IV. Application to processed foods, Food Hydrocoll. 6 (6) (1993) 503–511.
[29] H. Ougiya, K. Watanabe, Y. Morinaga, F. Yoshinaga, Emulsion-stabilizing effect of bacterial cellulose, Biosci. Biotechnol. Biochem. 61 (9) (1997) 1541–1545.
[30] H. Zhu, S. Jia, H. Yang, W. Tang, Y. Jia, Z. Tan, Characterization of bacteriostatic sausage casing: a composite of bacterial cellulose embedded with ε-polylysine, Food Sci. Biotechnol. 19 (6) (2010) 1479–1484.

[31] P. Paximada, E. Tsouko, N. Kopsahelis, A.A. Koutinas, I. Mandala, Bacterial cellulose as stabilizer of o/w emulsions, Food Hydrocoll. 53 (2016) 225–232.
[32] P. Paximada, A.A. Koutinas, E. Scholten, I.G. Mandala, Effect of bacterial cellulose addition on physical properties of WPI emulsions. Comparison with common thickeners, Food Hydrocoll. 54 ((2016) 245–254.
[33] M. Phisalaphong, N. Chiaoprakobkij, Applications and Products—Nata de Coco, Bacterial Cellulose: A Sophisticated Multifunctional Material, vol. 9, 2012 143–156.
[34] S. Cho, N. Almeida, Dietary Fiber and Health, CRC Press, 2012.
[35] K. Lin, H. Lin, Quality characteristics of Chinese-style meatball containing bacterial cellulose (Nata), J. Food Sci. 69 (3) (2004) SNQ107–SNQ111.
[36] S.B. Lin, L.C. Chen, H.H. Chen, Physical characteristics of surimi and bacterial cellulose composite gel, J. Food Process Eng. 34 (4) (2011) 1363–1379.
[37] R. Jonas, L.F. Farah, Production and application of microbial cellulose, Polym. Degrad. Stab. 59 (1–3) (1998) 101–106.
[38] A. Kuijk, R. Koppert, P. Versluis, G. van Dalen, C. Remijn, J. Hazekamp, J. Nijsse, K.P. Velikov, Dispersions of attractive semiflexible fiberlike colloidal particles from bacterial cellulose microfibrils, Langmuir 29 (47) (2013) 14356–14360.
[39] S.J. Veen, A. Kuijk, P. Versluis, H. Husken, K.P. Velikov, Phase transitions in cellulose microfibril dispersions by high-energy mechanical deagglomeration, Langmuir 30 (44) (2014) 13362–13368.
[40] S.J. Veen, P. Versluis, A. Kuijk, K.P. Velikov, Microstructure and rheology of microfibril–polymer networks, Soft Matter 11 (46) (2015) 8907–8912.
[41] Y. Huang, C. Zhu, J. Yang, Y. Nie, C. Chen, D. Sun, Recent advances in bacterial cellulose, Cellulose 21 (1) (2014) 1–30.
[42] A.M.A. Gallegos, S.H. Carrera, R. Parra, T. Keshavarz, H.M. Iqbal, Bacterial cellulose: a sustainable source to develop value-added products–a review, Bioresources 11 (2) (2016) 5641–5655.
[43] Z. Shi, Y. Zhang, G.O. Phillips, G. Yang, Utilization of bacterial cellulose in food, Food Hydrocoll. 35 (2014) 539–545.
[44] C. Ersch, M.B.J. Meinders, W.G. Bouwman, M. Nieuwland, E. van der Linden, P. Venema, A.H. Martin, Microstructure and rheology of globular protein gels in the presence of gelatin, Food Hydrocoll. 55 (2016) 34–46.
[45] V. Schuh, K. Allard, K. Herrmann, M. Gibis, R. Kohlus, J. Weiss, Impact of carboxymethyl cellulose (CMC) and microcrystalline cellulose (MCC) on functional characteristics of emulsified sausages, Meat Sci. 93 (2) (2013) 240–247.
[46] V. Urbonaite, H.H.J. de Jongh, E. van der Linden, L. Pouvreau, Origin of water loss from soy protein gels, J. Agric. Food Chem. 62 (30) (2014) 7550–7558.
[47] Y. Chung, Y. Shyu, The effects of pH, salt, heating and freezing on the physical properties of bacterial cellulose—nata, Int. J. Food Sci. Technol. 34 (1) (1999) 23–26.
[48] S.M. Fitzsimons, D.M. Mulvihill, E.R. Morris, Denaturation and aggregation processes in thermal gelation of whey proteins resolved by differential scanning calorimetry, Food Hydrocoll. 21 (4) (2007) 638–644.
[49] J.I. Boye, I. Alli, A.A. Ismail, B.F. Gibbs, Y. Konishi, Factors affecting molecular characteristics of whey protein gelation, Int. Dairy J. 5 (4) (1995) 337–353.
[50] M.M. Ould Eleya, S.L. Turgeon, Rheology of κ-carrageenan and β-lactoglobulin mixed gels, Food Hydrocoll. 14 (1) (2000) 29–40.
[51] W.S. Gosal, A.H. Clark, S.B. Ross-Murphy, Fibrillar β-lactoglobulin gels: part 2. Dynamic mechanical characterization of heat-set systems, Biomacromolecules 5 (6) (2004) 2420–2429.
[52] A. Clark, 3 Gelation of globular proteins, Functional Properties of Food Macromolecules (1) 1998, p. 77.
[53] M. Stading, A.-M. Hermansson, Large deformation properties of β-lactoglobulin gel structures, Food Hydrocoll. 5 (4) (1991) 339–352.
[54] G. Agoda-Tandjawa, S. Durand, C. Gaillard, C. Garnier, J.L. Doublier, Rheological behaviour and microstructure of microfibrillated cellulose suspensions/low-methoxyl pectin mixed systems. Effect of calcium ions, Carbohydr. Polym. 87 (2) (2012) 1045–1057.
[55] M. Beaulieu, S.L. Turgeon, J.-L. Doublier, Rheology, texture and microstructure of whey proteins/low methoxyl pectins mixed gels with added calcium, Int. Dairy J. 11 (11−12) (2001) 961–967.
[56] C. Ersch, I. ter Laak, E. van der Linden, P. Venema, A. Martin, Modulating fracture properties of mixed protein systems, Food Hydrocoll. 44 (2015) 59–65.
[57] A. Clark, G. Kavanagh, S. Ross-Murphy, Globular protein gelation—theory and experiment, Food Hydrocoll. 15 (4) (2001) 383–400.
[58] P.B. Fernandes, Viscoelastic characteristics of whey protein systems at neutral pH, Food Hydrocoll. 8 (3) (1994) 277–285.
[59] J. Peng, V. Calabrese, S.J. Veen, P. Versluis, K.P. Velikov, P. Venema, E. van der Linden, Rheology and microstructure of dispersions of protein fibrils and cellulose microfibrils, Food Hydrocoll. 82 (2018) 196–208.
[60] M. Langton, A.-M. Hermansson, Fine-stranded and particulate gels of β-lactoglobulin and whey protein at varying pH, Food Hydrocoll. 5 (6) (1992) 523–539.
[61] W. Chantrapornchai, D.J. McClements, Influence of NaCl on optical properties, large-strain rheology and water holding capacity of heat-induced whey protein isolate gels, Food Hydrocoll. 16 (5) (2002) 467–476.
[62] E.A. Foegeding, E.L. Bowland, C.C. Hardin, Factors that determine the fracture properties and microstructure of globular protein gels, Food Hydrocoll. 9 (4) (1995) 237–249.
[63] V. Urbonaite, S. van der Kaaij, H. de Jongh, E. Scholten, K. Ako, E. van der Linden, L. Pouvreau, Relation between gel stiffness and water holding for coarse and fine-stranded protein gels, Food Hydrocoll. 56 (2016) 334–343.
[64] S.-B. Lin, L.-C. Chen, H.-H. Chen, Physical characteristics of surimi and bacterial cellulose composite gel, J. Food Process Eng. 34 (4) (2011) 1363–1379.
[65] A. Okiyama, M. Motoki, S. Yamanaka, Bacterial cellulose III. Development of a new form of cellulose, Food Hydrocoll. 6 (6) (1993) 493–501.